Sanguinarine Biosynthesis Is Associated with the Endoplasmic Reticulum in Cultured Opium Poppy Cells after Elicitor Treatment[1]

Joenel Alcantara[2], David A. Bird[2,3], Vincent R. Franceschi, and Peter J. Facchini*

Department of Biological Sciences, University of Calgary, Calgary, Alberta, Canada T2N 1N4
(J.A., D.A.B., P.J.F.); and School of Biological Sciences, Washington State University, Pullman,
Washington 99164–4236 (V.R.F.)

Three key benzylisoquinoline alkaloid biosynthetic enzymes, (S)-N-methylcoclaurine-3′-hydroxylase (CYP80B1), berberine bridge enzyme (BBE), and codeinone reductase (COR), were localized in cultured opium poppy (Papaver somniferum) cells by sucrose density gradient fractionation and immunogold labeling. CYP80B1 catalyzes the second to last step in the formation of (S)-reticuline, the last common intermediate in sanguinarine and morphine biosynthesis. BBE converts (S)-reticuline to (S)-scoulerine as the first committed step in sanguinarine biosynthesis, and COR catalyzes the penultimate step in the branch pathway leading to morphine. Sanguinarine is an antimicrobial alkaloid that accumulates in the vacuoles of cultured opium poppy cells in response to elicitor treatment, whereas the narcotic analgesic morphine, which is abundant in opium poppy plants, is not produced in cultured cells. CYP80B1 and BBE were rapidly induced to high levels in response to elicitor treatment. By contrast, COR levels were constitutive in the cell cultures, but remained low and were not induced by addition of the elicitor. Western blots performed on protein homogenates from elicitor-treated cells fractionated on a sucrose density gradient showed the cosedimentation of CYP80B1, BBE, and sanguinarine with calreticulin, and COR with glutathione S-transferase. Calreticulin and glutathione S-transferase are markers for the endoplasmic reticulum (ER) and the cytosol, respectively. In response to elicitor treatment, large dilated vesicles rapidly developed from the lamellar ER of control cells and fused with the central vacuole. Immunogold localization supported the association of CYP80B1 and BBE with ER vesicles, and COR with the cytosol in elicitor-treated cells. Our results show that benzylisoquinoline biosynthesis and transport to the vacuole are associated with the ER, which undergoes major ultrastructural modification in response to the elicitor treatment of cultured opium poppy cells.

Alkaloids are a diverse group of approximately 12,000 low molecular weight, nitrogen-containing compounds found in about 20% of plant species. Morphine and sanguinarine are members of the large and diverse group of benzylisoquinoline alkaloids, of which more than 2,500 different structures have been identified in plants. Although morphine is a potent narcotic analgesic, it has been implicated in the stress-induced cross-linking of galacturonic-containing polysaccharides in the cell walls of opium poppy (Papaver somniferum) plants (Morimoto et al., 2001). By contrast, sanguinarine, which shows specific toxic effects to herbivores and microbial pathogens, is proposed to function as an inducible defense compound

(Schmeller et al., 1997). Benzylisoquinoline alkaloids share a common biosynthetic pathway, beginning with the condensation of two L-Tyr derivatives to produce the central precursor (S)-norcoclaurine (Fig. 1; Samanani et al., 2004). Specific O- and N-methyltransferases convert (S)-norcoclaurine to (S)-N-methylcoclaurine (Facchini, 2001). The P450-dependent monooxygenase (S)-N-methylcoclaurine-3′-hydroxylase (CYP80B1) catalyzes the 3′-hydroxylation of (S)-N-methylcoclaurine (Pauli and Kutchan, 1998). The subsequent 4′-O-methylation of (S)-3′-hydroxy-N-methylcoclaurine yields (S)-reticuline, the last common intermediate in the biosynthesis of both sanguinarine and morphine (Facchini, 2001). The berberine bridge enzyme (BBE) catalyzes the conversion of (S)-reticuline to (S)-scoulerine, the first committed step in the sanguinarine pathway (Facchini et al., 1996b). Alternatively, (S)-reticuline can be isomerized to its (R)-epimer as the first step in the formation of morphine (Fig. 1). The NADPH-dependent enzyme codeinone reductase (COR) converts (−)-codeinone to (−)-codeine as the penultimate step in morphine biosynthesis (Unterlinner et al., 1999). Sanguinarine is produced in cultured opium poppy cells in response to treatment with a fungal-derived elicitor (Facchini et al., 1996a). By contrast, morphine accumulation has not been detected in

induced or noninduced cell cultures, although both alkaloids are abundant in the plant.

Many alkaloid biosynthetic enzymes are found in subcellular compartments other than the cytosol. For example, enzymes of the monoterpenoid indole alkaloid pathway in *Catharanthus roseus* have been localized to the cytosol (De Luca and Cutler, 1987), vacuole (McKnight et al., 1991), tonoplast (Stevens et al., 1993), thylakoid membranes (De Luca and Cutler, 1987), and endoplasmic reticulum (ER; St-Pierre and De Luca, 1995). The involvement of multiple subcellular compartments is also apparent in the biosynthesis of quinolizidine alkaloids. Although the quinolizidine nucleus is synthesized in chloroplasts (Wink and Hartmann, 1982), subsequent modifications occur only after alkaloid intermediates are transported to the cytosol and mitochondria. Two acyltransferases that catalyze the acylation of (+)-*p*-coumaroylepilupinine and (−)-13α-tigloyloxymultifluorine were differentially localized to the cytoplasm and mitochondria, respectively, of *Lupinus albus* (Suzuki et al., 1996). Ultimately, quinolizidine alkaloids are thought to accumulate in the vacuoles of epidermal cells where their defensive properties can be most effective. Such complex schemes for the compartmentalization of metabolic enzymes effectively sequester toxic alkaloids and biosynthetic intermediates away from the cytosol. The subcellular trafficking of pathway intermediates also creates a potentially key level of metabolic regulation that would not be possible if enzymes and substrates diffused freely in the cytosol.

In cultured cells, five enzymes involved in the conversion of (*S*)-reticuline to dihydrosanguinarine have been associated with a subcellular compartment other than the cytosol. BBE and three subsequent P450-dependent monooxygenases were localized to a membrane fraction with a specific density (δ) of 1.14 g mL^{-1} (Amann et al., 1986; Rueffer and Zenk, 1987; Bauer and Zenk, 1989, 1991). A fourth P450-dependent enzyme was detected in microsomes with a δ of 1.11 g mL^{-1}, consistent with the expected density of the ER (Tanahashi and Zenk, 1990). Eukaryotic P450-dependent enzymes, such as CYP80B1, are typically anchored to the ER by an N-terminal insertion and stop transfer peptide (Sakaguchi et al., 1987), but have also been reported to target mitochondria (Ogishima and Okada, 1985; Neve and Ingelman-Sundberg, 2001) and chloroplasts (Pan et al., 1995; Froehlich et al., 2001). CYP80B1 from opium poppy contains a noncleavable N-terminal ER-signal peptide (Nielsen et al., 1997; Nakai and Horton, 1999) according to SignalP and PSORT prediction software analysis, suggesting the cotranslational targeting to the ER in a manner similar to mammalian P450-dependent enzymes (Sakaguchi et al., 1987).

The cosedimentation of some benzylisoquinoline alkaloid biosynthetic enzymes with an endomembrane fraction exhibiting a density greater than that of the ER has led to speculation that distinct alkal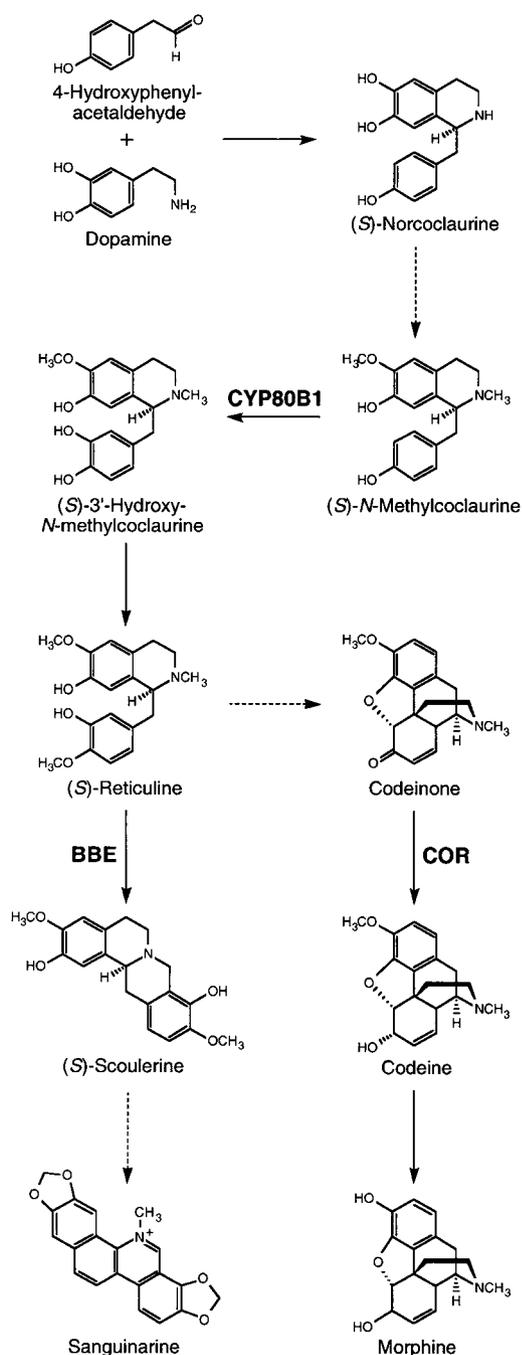oid-synthesizing vesicles occur in certain cell types (Amann et al., 1986). Vesicles with a δ of 1.14 g mL^{-1} and containing various alkaloids and biosynthetic enzymes have been visualized within vacuole-like compartments (Amann et al., 1986). Moreover, nascent BBE was found to contain a targeting domain composed of an N-terminal signal peptide and an adjacent vacuolar-sorting determinant (Bird and Facchini, 2001). The predicted inactivation of BBE by the acidity of the vacuole suggests that alkaloid biosynthesis occurs before the enzyme crosses the tonoplast. The purported vacuolar accumulation of sanguinarine (Kutchan et al., 1986) implies that the entire contents of the transport vesicles, including biosynthetic enzymes and various alkaloid metabolites, might be translocated from the ER to the vacuole.

In this study, we investigate the subcellular localization of CYP80B1, BBE, and COR as representative enzymes of benzylisoquinoline alkaloid biosynthesis in cultured opium poppy cells treated with a fungal elicitor. We show that the association of CYP80B1 and BBE with the ER is correlated with major changes in ER ultrastructure, which appear to be linked to the elicitor-induced biosynthesis of sanguinarine in cultured opium poppy cells. Suc density gradient fractionation was used to show the localization of benzylisoquinoline alkaloid biosynthetic enzymes with distinct subcellular compartments, which were identified using antibodies to CYP80B1, BBE, COR, and specific marker proteins. Immunogold labeling and electron microscopy were used to support the subcellular compartmentalization of each biosynthetic enzyme and document changes in the ultrastructure in cultured opium poppy cells in response to elicitor treatment.

RESULTS

CYP80B1, BBE, and COR Levels in Elicited Opium Poppy Cell Cultures

A time-course experiment was performed on opium poppy cell cultures treated with *Botrytis cinerea* fungal homogenate to determine if CYP80B1, BBE, and COR enzyme levels change in response to elicitor treatment. Protein was extracted from control cell cultures collected immediately after elicitor treatment (i.e. 0 h) and at various time points thereafter. Western-blot analysis was performed on these extracts using anti-CYP80B1, anti-BBE, anti-COR, and anti-calreticulin antibodies (Fig. 2). CYP80B1 and BBE protein levels were not detectable in control extracts but began to increase 5 h after the addition of the elicitor (Fig. 2). Although the levels of both CYP80B1 and BBE increased in response to elicitor treatment, BBE levels peaked at 50 h, whereas CYP80B1 levels continued to rise until at least 80 h postelicitation (Fig. 2). By contrast, COR and calreticulin were detected in control cultures, and their levels did not change in response to the addition of the elicitor (Fig. 2).

Western blots were performed on selected fractions using antibodies specific to calreticulin, glutathione S-transferase (GST), mitochondrial aldehyde dehydrogenase (RF2), and plasma membrane proton-ATPase (PM H$^+$-ATPase), which represented markers for the ER (Campos et al., 1996), cytosol (Marrs, 1996), mitochondria (Quitadamo et al., 2000), and plasma membrane (Liu et al., 2001), respectively. Calreticulin and PM H$^+$-ATPase levels peaked in fractions with specific densities of 1.12 and 1.09 g mL^{-1}, respectively (Fig. 3). By contrast, GST and RF2 were most abundant in fractions with lower (1.05–1.07 g mL^{-1}) and higher (1.20–1.22 g mL^{-1}) specific densities, respectively, compared with calreticulin and PM H$^+$-ATPase (Fig. 3). Using specific antibodies, CYP80B1 and BBE cofractionated with calreticulin (1.10–1.12 g mL^{-1}), whereas COR was detected in the same fractions as GST (Fig. 3). Moreover, sanguinarine was also found to cofractionate with calreticulin, CYP80B1, and BBE (Fig. 3). Identical results were obtained with opium poppy cells treated with the elicitor for 50 h (data not shown). Freezing and thawing the cell homogenate prior to loading onto the Suc density gradient caused the disruption of membranous compartments and abolished the cofractionation of calreticulin with BBE and sanguinarine, which were instead primarily associated with the fractions containing GST (data not shown).

Magnesium/EDTA Shift Assay of Elicited Opium Poppy Cell Cultures

Suc density gradients were prepared with either 10 mM MgSO$_4$ or 10 mM EDTA to distinguish between microsomal fractions containing calreticulin and plasma membrane vesicles containing PM H$^+$-ATPase. Magnesium ions maintain the binding of ribosomes to the ER surface, thus increasing its density. Conversely, addition of the chelating agent EDTA strips ribosomes from the ER, thus decreasing its density (Lord, 1983). In

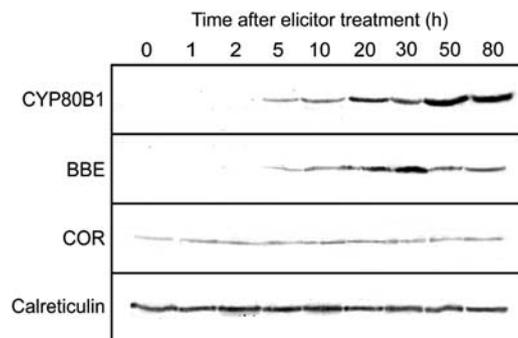**Figure 1.** Conversions catalyzed by CYP80B1, BBE, and COR in the biosynthesis of sanguinarine and morphine.

Suc Density Gradient Fractionation of Elicited Opium Poppy Cell Cultures

Protein homogenates from opium poppy cell cultures treated with the elicitor for 30 h were fractionated on a 15% to 65% continuous Suc density gradient to determine the subcellular localization of CYP80B1, BBE, and COR (Fig. 3). After ultracentrifugation, 1-mL fractions were collected from the bottom of the tube, and the density of each fraction was determined.


Figure 2. Time course showing the induction of CYP80B1, BBE, and COR protein levels in cultured opium poppy cells treated with a fungal elicitor. Total cellular proteins were extracted, fractionated on by SDS-PAGE, and transferred to nitrocellulose membranes. Specific proteins were detected on western blots using antibodies raised against CYP80B1, BBE, COR, or calreticulin. Blots are representative of three independent experiments.
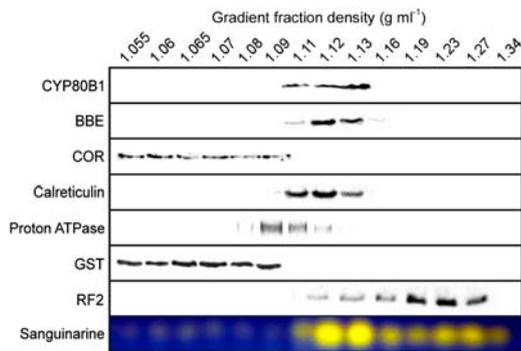
Figure 3. Suc density gradient fractionation of cultured opium poppy cells treated with a fungal elicitor for 30 h. Every second fraction recovered from the gradient was used. Results are representative of three independent experiments.

the presence of 10 mM $MgSO_4$, calreticulin was found in Suc gradient fractions with densities between 1.14 and 1.18 g mL^{-1}, whereas in the presence of EDTA calreticulin localized to gradient fractions with densities between 1.09 and 1.11 g mL^{-1} (Fig. 4). CYP80B1, BBE, and sanguinarine cosedimented with calreticulin in Suc density gradients containing EDTA or $MgSO_4$ (Fig. 4). By contrast, the PM H$^+$-ATPase did not shift to more dense fractions in the presence of $MgSO_4$, nor did it shift to less dense fractions in EDTA-containing gradients (Fig. 4). The densities of each fraction were plotted as a function of fraction number to confirm that the two gradients were linear and similar (data not shown).

Ultrastructural Changes in Opium Poppy Cells after Elicitor Treatment

A time-course experiment was performed to identify changes in the cellular ultrastructure of cultured opium poppy cells in response to elicitor treatment (Fig. 5). Using a standard aldehyde fixation protocol for transmission electron microscopy, the actively growing control cultured cells were seen to have a dense cytoplasm, several plastids, and many mitochondria (Fig. 5A). Within 5 h after the addition of the elicitor, some cells showed the presence of large vesicles in the cytoplasm that were not typical of control cells (Fig. 5C). After 10 h there was evidence that smaller vesicles had fused to form large vesicles (Fig. 5D), and by 50 h the movement of vesicles to the tonoplast was apparent (Fig. 5E). The larger vesicles were often seen projecting into the vacuoles (Fig. 5, D and E). Eighty hours after elicitor treatment, many cells showed an apparent hypersensitive response including disruption of the cytoplasm and the presence of multivesicular bodies (Fig. 5F). In the later time points after elicitor treatment, the abundance of a flocculent material in the vacuole also increased, although it did not stain well using aldehyde fixation (Fig. 5E).

Potassium permanganate fixation produces a high contrast of membranous structures in cells as viewed by transmission electron microscopy, and was used to better establish endomembrane dynamics within the elicitor-treated opium poppy cell cultures. Numerous organelles and a distinctive lamellar ER were evident in control cells prepared with this fixation protocol (Fig. 6A). This fixation technique clearly showed a proliferation of irregularly shaped vesicles in the cytoplasm of elicitor-treated cells, and these vesicles contained an electron-dense material (Fig. 6B). A similar electron-dense, flocculent material was seen to accumulate in the vacuole of elicitor-treated cells (Fig. 6B). Control cells contained relatively little electron-dense material in the central vacuole and the ER lumen (Fig. 6A). Examination of many cells indicated that the large vesicles in elicitor-treated cells appeared to result from dilations of lamellar ER (Fig. 6C). The vesicles were often closely associated with the tonoplast of the central vacuole (Fig. 6B). Flocculent, electron-dense material was not visible in the Golgi of either control or elicited cells (data not shown).

Cultured opium poppy cells fixed using high-pressure freezing and freeze substitution also showed the formation of large vesicles in response to elicitor treatment (Fig. 6, D to F). Membranes of the large vesicles and the tonoplast were lined with an electron-dense material in elicitor-treated cells (Fig. 6E). In control cells, the ER exhibited a lamellar structure and together with the tonoplast lacked an electron-dense membrane lining (Fig. 6D). The large, dilated ER vesicles appeared to fuse with the central vacuole since vesicles were frequently found near the tonoplast (Fig. 6E) and complete fusion was sometimes detected (Fig. 6F).

Immunogold Localization of CYP80B1, BBE, and COR

To support the localization of CYP80B1 and BBE to the ER, and COR to the cytosol, as suggested by Suc density gradient fractionation experiments (Figs. 3 and
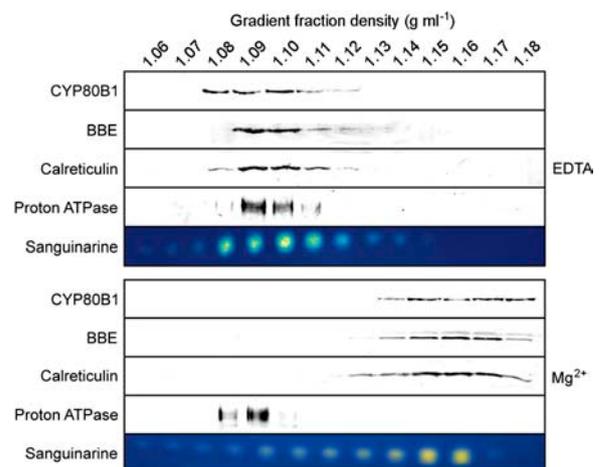

Figure 4. Suc density gradient fractionation, in the presence of magnesium or EDTA, of opium poppy cells treated with a fungal elicitor for 30 h. Every second fraction recovered from the gradient was used. Results are representative of three independent experiments.
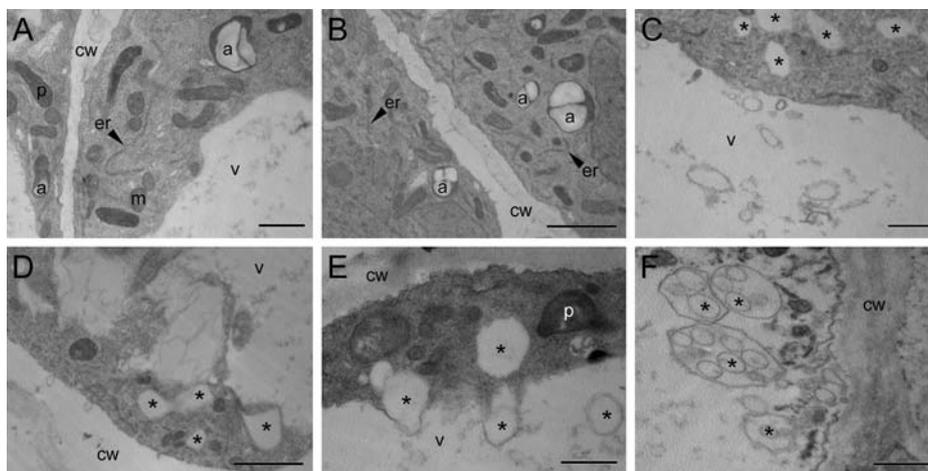
Figure 5. Time course of osmium tetroxide-fixed cultured opium poppy cells treated with a fungal elicitor. A, Control cell. B to F, Cells at different times after elicitor treatment: B, 2 h; C, 5 h; D, 10 h; E, 50 h; and F, 80 h. The actively growing control cells have a dense cytoplasm, and many plastids and mitiochondria (A). By 5 h posttreatment, some cells show the presence of large vesicles in the cytoplasm (C). After 10 h, there is evidence of smaller vesicles fusing to form large vesicles (D), and by 50 h the movement of vesicles to the tonoplast is apparent (E). Eighty hours after treatment, many cells show disruption of the cytoplasm and the presence of multivesicular bodies (F). Asterisks show the location of large cytoplasmic vesicles. Abbreviations are as follows: a, amyloplasts; cw, cell wall; er, endoplasmic reticulum; m, mitochondrion; p, plastid; and v, vacuole. Bars = 500 nm.

4), antibodies specific to each protein were used for immunogold localization in opium poppy cells treated with a fungal elicitor for 50 h. CYP80B1 was associated with the periphery of the ER, and labeling was not found in association with any other cellular compartment (Fig. 7A). Label for BBE was also detected along the ER and not in other locations (Fig. 7B). While labeling was along the ER in both cases, it could not be determined if the labeled proteins were on a particular surface of the ER or in the lumen. During tissue
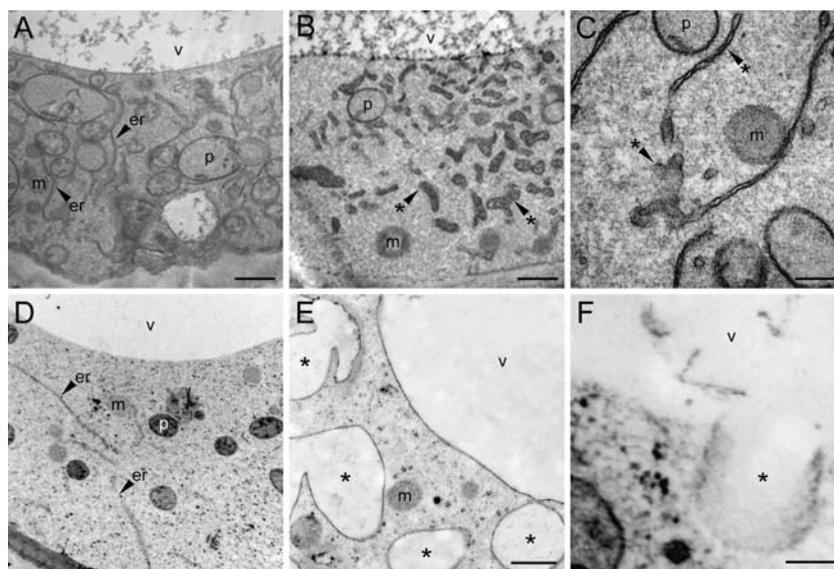
Figure 6. Permanganate-fixed (A–C), and high-pressure frozen and freeze-substituted (D–F) cultured opium poppy cells. A, Permanganate-fixed control cell showing extensive lamellar ER but lacking large vesicles. B, Permanganate-fixed cultured cell 50 h after elicitor treatment showing proliferation of large cytoplasmic vesicles containing a flocculent, electron-dense material, which also appears in the vacuole. C, Permanganate-fixed cultured cell 50 h after elicitor treatment showing dilations of lamellar ER, which develop into larger vesicles with flocculent material. D, High-pressure frozen and freeze-substituted control cell showing extensive lamellar ER but lacking large vesicles. E, High-pressure frozen and freeze-substituted cultured cell 50 h after elicitor treatment showing large cytoplasmic vesicles with an electron-dense membrane lining. Note the proximity of vesicle with tonoplast at bottom right of image. F, High-pressure frozen and freeze-substituted cultured cell 50 h after elicitor treatment showing the fusion of a large cytoplasmic vesicle with the central vacuole. Asterisks show the locations of large cytoplasmic vesicles. Abbreviations are as follows: cw, cell wall; m, mitochondrion; p, plastid; and v, vacuole. Bars = 500 nm.
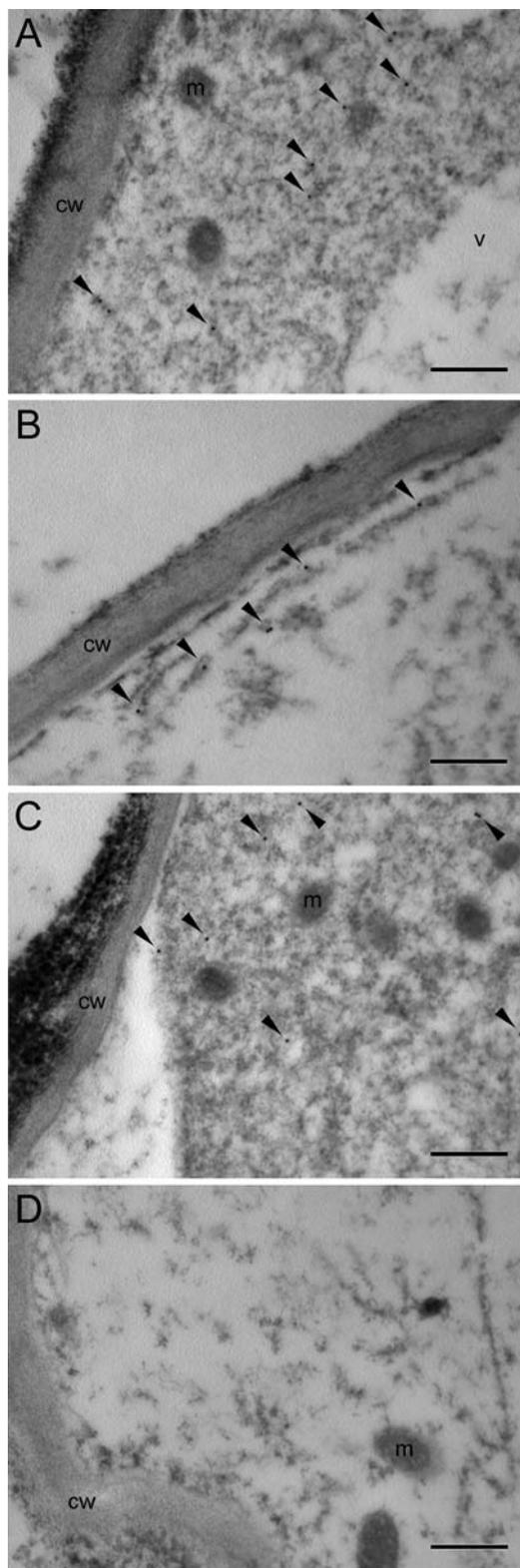
preparation, even lumenal proteins can become adsorbed to the ER membrane, and the resolution of the technique, as used, was also not sufficient to definitively determine on which side of the membrane an immunoreactive protein might reside (Fig. 7B). COR was localized throughout the cytosol and was not associated with the ER or other organelles (Fig. 7C). Cell sections treated with preimmune serum from individual mice used to produce the anti-CYP80B1, anti-BBE, or anti-COR sera did not show labeling (Fig. 7D).
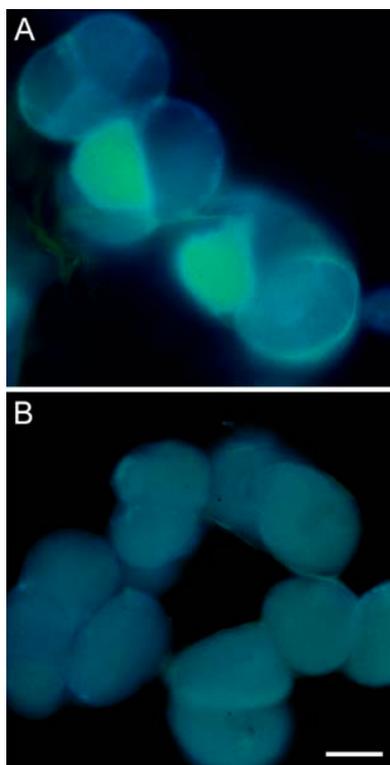
Sanguinarine Accumulation in Elicitor-Treated Opium Poppy Cell Cultures

The fluorescent alkaloid sanguinarine was found to accumulate in the central vacuole of only approximately 20% of cultured opium poppy cells in response to elicitor treatment (Fig. 8). Moreover, only cells physically associated with other cultured cells were found to contain detectable amounts of sanguinarine.

DISCUSSION

The accumulation of benzylisoquinoline alkaloids in elicitor-treated opium poppy cell cultures involves the transcriptional activation of all known genes involved in the biosynthesis of (S)-reticuline and sanguinarine (Facchini and Park, 2003). Time-course experiments to examine the induction of CYP80B1 and BBE protein levels (Fig. 2) were in temporal agreement with the accumulation of corresponding gene transcripts (Huang and Kutchan, 2000; Facchini and Park, 2003). COR was present in noninduced cells, but did not increase in response to elicitor treatment at the transcriptional (Huang and Kutchan, 2000; Facchini and Park, 2003) or posttranslational (Fig. 2) levels. Despite the general occurrence of several morphine biosynthetic enzymes in opium poppy cell cultures (Gerardy and Zenk, 1993a, 1993b; Lenz and Zenk, 1995a, 1995b), products of this branch pathway are not produced. The inability of cultured opium poppy cells to accumulate morphine might be caused by the absence of other relevant enzymes. The silencing of *COR* genes in transgenic opium poppy plants resulted in the accumulation of (S)-reticuline rather than codeinone (Allen et al., 2004). Thus, the absence of a single enzyme prevents intermediates from general benzylisoquinoline alkaloid biosynthesis from entering the morphine-specific branch pathway. Nevertheless, the efficient operation of the sanguinarine pathway shows that cultured opium poppy cells possess the essential regulatory, cellular, and metabolic components to

Figure 7. Immunogold localization of CYP80B1, BBE, and COR in cultured opium poppy cells treated with a fungal elicitor for 50 h. A, Anti-CYP80B1 serum. Labeling is associated with the ER (arrowheads). B, Anti-BBE. Labeling is associated with the ER. C, Anti-COR serum. Labeling is associated with the cytosol. D, Preimmune serum from the mouse used to produce anti-CYP80B1 serum. No labeling is visible. Ten-

nanometer, gold-conjugated IgGs (anti-mouse or anti-rabbit, as appropriate) were used as the secondary antibodies in all cases. Abbreviations are as follows: v, vacuole; m, mitochondrion; and cw, cell wall. Bars = 500 nm.

Figure 8. Autofluorescence of control and elicitor-treated opium poppy cell cultures. A, Cultured cell 50 h after elicitor treatment poppy cells showing distinct yellow-green fluorescence due to the accumulation of sanguinarine in the vacuoles. Only some of the cells show this fluorescence. B, Noninduced cells in which yellow-green fluorescence is not visible. Bar = 25 μm.

support the biosynthesis and accumulation of a highly substituted and cytotoxic benzylisoquinoline alkaloid.

Our results show that sanguinarine biosynthesis occurs in association with the ER of cultured opium poppy cells in response to elicitor treatment. CYP80B1, BBE, and sanguinarine were shown to cosediment with calreticulin by Suc density gradient fractionation (Figs. 3 and 4). The cellular fractionation-based localization of CYP80B1 and BBE to the ER was supported by the immunogold labeling of elicitor-treated opium poppy cell cultures (Fig. 7). CYP80B1 is an integral membrane protein associated with an ER-bound NAD(P)H-dependent cytochrome P450 reductase (Pauli and Kutchan, 1998). By contrast, the association of BBE and sanguinarine with the ER did not involve lipophilic interactions since successive freezing and thawing of the Suc density gradient fractions caused the release of these components, but not CYP80B1, into lower density cytosolic fractions (data not shown). Nascent BBE has been shown to contain a cleaved N-terminal signal peptide and reside as a soluble protein within discrete ER-derived compartments (Amann et al., 1986; Galneder et al., 1988; Bird and Facchini, 2001). The localization of COR to the cytosol was also demonstrated using a combination of Suc density gradient

fractionation and immunogold labeling (Figs. 3 and 7). Although COR is a soluble enzyme and lacks a signal peptide, the localization of the morphine branch pathway to the cytosol is not expected due to the general cytotoxicity of benzylisoquinoline alkaloids.

The putative improper compartmentalization of COR might reflect the inability of cultured opium poppy cells to form a complex of morphine branch pathway enzymes (Allen et al., 2004). BBE was previously shown to contain a vacuolar-sorting determinant adjacent to the signal peptide (Bird and Facchini, 2001). The function of this motif might involve the targeting of BBE to a specific subdomain of the ER, perhaps via interactions with other proteins involved in sanguinarine biosynthesis. Multienzyme complexes have been demonstrated for flavonoid (Burbulis and Winkel-Shirley, 1999; He and Dixon, 2000; Achnine et al., 2004) and polyamine (Panicot et al., 2002) metabolism in Arabidopsis (*Arabidopsis thaliana*). Such complexes involve physical interactions between successive biosynthetic enzymes, which allow the efficient and isolated channeling of intermediates along a metabolic pathway. The ultimate sequestration of polypeptide fusions between N-terminal domains of BBE and the green fluorescent protein to the vacuole of cultured opium poppy cells (Bird and Facchini, 2001) appears to reflect the association of BBE with ER-derived vesicles (Figs. 3, 4, and 7) and the transport of these vesicles to the vacuole (Fig. 6). Using immunogold labeling, (*S*)-tetrahydroprotoberberine oxidase polypeptides were also detected in association with cytoplasmic vesicles, in addition to electron-dense deposits in the vacuole, and material along the vacuolar surface of the tonoplast in cultured *Berberis wilsoniae* cells (Bock et al., 2002). (*S*)-Tetrahydroprotoberberine oxidase catalyzes the last step in berberine biosynthesis, which also involves the activities of CYP80B1 and BBE, and the apparent migration of cytoplasmic vesicles to the central vacuole.

Potassium permanganate fixation showed the accumulation of a flocculent material in ER-derived vesicles and the central vacuole after elicitor treatment (Fig. 6). The flocculent material was not proteinaceous due to the strong oxidizing properties of potassium permanganate, which results in low contrast of protein-rich constituents, such as ribosomes and the cytoskeleton (Giddings, 2003). Moreover, a flocculent, electron-dense material was also formed by the addition of 2% (w/v) potassium permanganate to isolated sanguinarine, but not by potassium permanganate and buffer alone. Using high-pressure freezing and freeze substitution, the membranes of ER-derived vesicles and the tonoplast were lined with an electron-dense deposit (Fig. 6, D and E), which might correspond to the flocculent material visible in potassium permanganate-fixed tissues (Fig. 6, A and B). Similar electron dense deposits have been reported in a variety of cell cultures that show a constitutive or inducible accumulation of benzylisoquinoline alkaloids (Eilert and Constabel, 1985; Amann et al., 1986;

Yamamoto et al., 1986; Cline and Coscia, 1989; Deliu et al., 1994; Bock et al., 2002).

The large vesicles in elicited opium poppy cells (Figs. 5 and 6) appeared similar in size and morphology to previously reported alkaloid-synthesizing vesicles (Amann et al., 1986; Galneder et al., 1988). Our results show that these alkaloid-synthesizing vesicles are not distinct organelles as previously suggested (Amann et al., 1986), but are simply dilations of the ER (Figs. 5 and 6). The predicted fusion or engulfment of benzylisoquinoline alkaloid-producing vesicular compartments with or by the central vacuole (Amann et al., 1986; Bird and Facchini, 2001; Bock et al., 2002) is supported by our ultrastructural data (Figs. 5 and 6). The sorting of ER domains to the vacuole and the formation of new organelles without the involvement of Golgi has been demonstrated in other systems. For example, direct biogenesis of peroxisomes is thought to occur via the sorting of peroxisomal proteins to ER subdomains, which subsequently form nascent vesicles (Johnson and Olsen, 2001; Mullen et al., 2001). Similarly, seed storage proteins accumulate within specialized nonacidic vacuoles, which develop directly from ER subdomains (Li et al., 1993; Jiang and Rogers, 1998).

The formation and storage of sanguinarine in cultured opium poppy cells appears to involve a similar process. Our data show that elicitor treatment causes the simultaneous activation of alkaloid biosynthetic gene expression and dilation of the ER. The induced biosynthetic enzymes can be detected by western-blot analysis (Fig. 2) and immunogold labeling (Fig. 7) during, and subsequent to, the dilation of large ER-derived vesicles (Figs. 5 and 6). Immunogold labeling provides equivocal support for the association of CYP80B1 and BBE with dilated ER (Fig. 7). Dilated ER is likely present in the immunogold-labeled cells, but is not visible because vacuoles and large vesicles are typically ruptured by the aldehyde fixation of cultured opium poppy cells (data not shown). The biosynthetic enzyme- and alkaloid-laden vesicles migrate to, and fuse with, the tonoplast membrane, releasing their contents into the vacuole (Fig. 6). Alternatively, vesicles might aggregate within, or be engulfed by, small vacuoles that subsequently fuse to the central vacuole (Fig. 5). This model appears to accurately describe the cell biology of benzylisoquinoline alkaloid biosynthesis in different species (Amann et al., 1986; Yamamoto et al., 1986; Cline and Coscia, 1989; Deliu et al., 1994; Bock et al., 2002). By contrast, such ultrastructural changes have not been associated with the biosynthesis of acridone and monoterpenoid indole alkaloids (Eilert et al., 1986, 1987).

In the plant, benzylisoquinoline alkaloid biosynthesis has been suggested to involve sieve elements of the phloem, whereas products of the pathway are known to accumulate in laticifers (Bird et al., 2003). The localization of CYP80B1, BBE, and sanguinarine to the ER in cultured opium poppy cells can be extrapolated to the corresponding parietal sieve element reticulum in the plant. The localization of the benzylisoquinoline alkaloid pathway to the parietal sieve element reticulum would prevent biosynthetic enzymes from translocation through the phloem. Moreover, the large, alkaloid-containing vesicles found in opium poppy laticifers are thought to result from dilations of the ER (Nessler and Mahlberg, 1977), similar to the formation of dilated ER in cultured cells (Fig. 5).

Opium poppy cell cultures are not physiologically homogenous since sanguinarine accumulates in only a subset of elicitor-treated cells (Fig. 8). The cell line used in this study was selected for its ability to produce copious quantities of sanguinarine in response to elicitor treatment, with up to 50% of the alkaloid secreted into the culture medium (Eilert and Constabel, 1985). The secretion of sanguinarine is not due to cell death since we estimated the viability of elicitor-treated cell cultures at greater than 95%, as determined using the fluorescein diacetate method (Widholm, 1972), even 80 h after treatment. The lack of uniform sanguinarine accumulation could be linked to one or more factors, including (1) the differential expression of alkaloid biosynthetic genes, (2) the differential expression of a plasma membrane-localized transporter involved in alkaloid secretion, or (3) the intercellular translocation of sanguinarine. Benzylisoquinoline alkaloid biosynthesis and accumulation involve multiple cell types in the plant but appear to occur in the same cell in culture. Our model for the cell biology of sanguinarine biosynthesis in cultured opium poppy cells provides a platform to understand the intra- and intercellular translocation of benzylisoquinoline alkaloid biosynthetic enzymes, intermediates, and/or products in more highly differentiated cells of the plant.

MATERIALS AND METHODS

Plant Cell Cultures

Cell cultures of opium poppy (*Papaver somniferum*; cell line 2009) were maintained under fluorescent light at 23°C on Gamborg 1B5C medium consisting of B5 salts and vitamins, 100 mg L^{-1} myoinositol, 1 g L^{-1} hydrolyzed casein, 20 g L^{-1} Suc, and 1 mg L^{-1} 2,4-dichlorophenoxyacetic acid. Cells were subcultured every 6 d using a 1:3 dilution of inoculum to fresh medium.

Elicitor Preparation

Fungal elicitors were prepared according to Eilert et al. (1985). Sections (1 cm^2) of mycelium grown on potato dextrose agar were used to inoculate 50 mL of 1B5C medium including supplements but lacking 2,4-dichlorophenoxyacetic acid. Mycelium cultures of *Botrytis cinerea* were grown at 120 rpm on a gyratory shaker at 22°C in the dark for 6 d. Mycelia and medium were homogenized with a Polytron (Brinkmann Instruments, Westbury, NY), autoclaved at 121°C for 20 min, and subsequently centrifuged under sterile conditions with the supernatant serving as elicitor. One milliliter of fungal homogenate was added to 50 mL of cell culture.

Heterologous Expression and Purification of Proteins

The opium poppy *CYP80B1* (Huang and Kutchan, 2000) and *BBE1* (Facchini et al., 1996b) open reading frames were inserted in-frame into

pET29 (Novagen, Madison, WI) and the constructs introduced into *Escherichia coli* strain BL21(DE3). The opium poppy *COR* (Unterlinner et al., 1999) open reading frame was inserted in-frame into pRSET and the constructs introduced into *E. coli* strain ER2566 (New England Biolabs, Beverly, MA). Heterologous expression was performed according to the pET29 manual. Briefly, 1 L of NZY broth (86 mM NaCl, 20 mM $MgSO_4$, 5 mg L^{-1} yeast extract, 10 mg L^{-1} casein hydrolysate) containing 50 mg L^{-1} kanamycin (pET29-BBE) or 25 mg L^{-1} ampicillin (pRSET-CYP80B1 and pRSET-COR) was inoculated with 5 mL of overnight bacterial culture and incubated at 37°C. At a density of $OD_{600} = 0.5$, the cultures were induced for 4 h with 400 μM isopropyl-β-D-thiogalactopyranoside. Cells were pelleted, resuspended in homogenization buffer (50 mM Tris-HCl, pH 7.5, 10 mM EDTA, 10 μM phenylmethylsulfonyl fluoride [PMSF], and 5 mM 2-mercaptoethanol), and ruptured using a French press (Spectronic Instruments, Rochester, NY). Cell debris and protein inclusion bodies were recovered by centrifugation. The rinsed pellet was solubilized in homogenization buffer containing 6 M urea, and the solution was passed through a 0.20-μm filter. Recombinant proteins were affinity purified using a Ni^{2+}-charged HiTrap column according to manufacturer's instructions (Pharmacia Biotech, Piscataway, NJ).

Preparation of Antibodies

Antibodies were prepared from purified antigens using repeated subcutaneous injections. Antigen proteins were dialyzed against 146 mM NaCl, resuspended at a concentration of 400 μg mL^{-1}, emulsified (1:1) with Freund's complete adjuvant, and 100 μL injected into mice. Booster injections were performed every 3 weeks until a sufficient titer was achieved.

Protein Extraction, Fractionation, and Western-Blot Analysis

Cultured cells were collected by vacuum filtration and ground under liquid nitrogen to a fine powder with a mortar and pestle in the presence of polyvinyl polypyrrolidone (100 mg g^{-1} of tissue). Ground tissues were suspended in extraction buffer (50 mM Tris-HCl, pH 7.5, 5 mM EDTA, 5 μM PMSF, and 5 mM 2-mercaptoethanol), incubated on ice for 30 min, and the supernatant collected by centrifugation at 10,000g for 10 min at 4°C. Protein concentrations were determined according to Bradford (1976) using bovine serum albumin (BSA) as a standard. Protein samples (25 μg) were fractionated by SDS-PAGE using 10.5% (w/v) polyacrylamide gels and transferred to nitrocellulose membranes. Protein blots were incubated with 10 μg mL^{-1} CYP80B1 antiserum, 5 μg mL^{-1} BBE antiserum, or 25 μg mL^{-1} COR antiserum for 3 h, washed in 20 mM Tris-HCl, pH 7.5, 150 mM NaCl, 0.1% (v/v) Tween-20 (TBST), and incubated for 2 h with alkaline phosphatase-conjugated anti-mouse secondary antibodies (Bio-Rad, Hercules, CA). The membranes were washed in TBST and developed in alkaline phosphatase buffer (100 mM Tris-HCl, pH 9.5, 100 mM NaCl, and 5 mM $MgCl_2$) containing 20 μM nitroblue tetrazolium and 20 μM 5-bromo-4-chloro-3-indolyl phosphate as substrates.

Suc Density Gradient Centrifugation

Continuous Suc density gradients were prepared by layering 5-mL aliquots of 50 mM Tricine-NaOH, pH 7.5, solutions containing 65, 57, 45, 37, 30, 23, and 15% (w/v) Suc in thin-wall ultracentrifuge tubes (Nalgene, Rochester, NY). Layered gradients were equilibrated for 24 h at 4°C. For magnesium-shift assays, Suc solutions were supplemented with 10 mM EDTA or 10 mM $MgSO_4$. Protoplasts were isolated by incubating 1 g (fresh weight) of cultured plant cells in 10 mL of hydrolysis buffer (400 mM mannitol, 3 mM MES-NaOH, pH 5.8), containing 2% (w/v) cellulase R-10 (Onozuka Biochemicals, Nishinomiya, Japan) and 1% (w/v) macerozyme R-10 (Onozuka), for 16 h. Protoplasts were filtered through a 44-μm nylon mesh, centrifuged at 300g, rinsed in hydrolysis buffer, and centrifuged again. The pellet was resuspended in homogenization buffer (330 mM sorbitol, 50 mM HEPES-NaOH, pH 7.0, 0.1 mM PMSF, 2 mM EDTA, and 0.005% [v/v] Nonidet P-40) to a concentration of 2 to 3 × 10^3 mL^{-1}, and protoplasts were disrupted in a Potter-Elveheim tissue grinder. Seven milliliters of protoplast lysate were layered onto the Suc density gradient and centrifuged for 3 h at 100,000g. The bottom of the ultracentrifuge tube was punctured with a 24-gauge hypodermic needle and 1-mL fractions were collected. The Suc density of each fraction was determined using a refractometer (Fisher Scientific, Loughborough, Leicestershire, UK).

Osmium Tetroxide Fixation

Cultured opium poppy cells were fixed for 10 min in 4% (v/v) glutaraldehyde in 0.1 M cacodylic buffer, pH 7, followed by 2 h in 2% (v/v) paraformaldehyde and 2.5% (v/v) glutaraldehyde in 0.1 M cocodylate buffer, pH 7.3, and 0.2 M Suc. After fixation, the cells were washed three times for 5 min in 0.1 M cocodylate buffer, pH 7.3, and 0.2 M Suc, and fixed with 2% (w/v) osmium tetroxide for 2 h. After fixation, the cells were washed three times for 5 min in water, stained with 1% (w/v) tannic acid for 2 h, washed three times for 5 min in water, and stained with 2% (w/v) uranyl acetate for 2 h. The cells were dehydrated using a 30%, 50%, 60%, 80%, 95%, and 100% (v/v) acetone series with incubations of 2 h in each solution, and infiltrated with Spurr's resin (Electron Microscopy Sciences, Fort Washington, PA) using a 1:4, 1:3, 1:2, 1:1, 2:1, and 3:1 (resin:acetone) series with incubations of 4 h in each solution. Samples were transferred to pure resin, cast into 1-mL plastic capsules, and incubated at 60°C for 16 h.

Potassium Permanganate Fixation

Cultured plant cells were immersed in fixative (2% potassium permanganate in 50 mM veronal buffer, pH 9.0) for 2 h and rinsed three times each for 15 min in 100 mM sodium barbituate buffer, pH 8.8. Sections were dehydrated and embedded in Spurr's resin in acetone using a 1:4, 1:3, 1:2, 1:1, 2:1, and 3:1 (resin:acetone) infiltration series with incubations of 4 h in each solution. Samples were transferred to pure resin, cast into 1-mL plastic capsules, and incubated at 60°C for 16 h.

High-Pressure Freezing and Freeze Substitution

Cultured plant cells were resuspended in 25% dextran (39,000 g mol^{-1}; w/v) and collected on a 30-μm nylon mesh. The cell slurry was transferred to gold sample holders that were dipped in 100 mg mL^{-1} lecithin in chloroform and allowed to dry. The holder was immediately frozen in a Balzers HPM 010 high-pressure freezer (Bal-tec, Balzers, Liechtenstein) and transferred to liquid nitrogen for storage. Sample holders were opened under liquid nitrogen and transferred to cryosubstitution vials containing 2% (w/v) osmium tetroxide and 8% (v/v) dimethoxypropane in anhydrous acetone. Cryosubstitution was performed at −80°C for 2 to 3 d in a bath of acetone and dry ice, and then slowly warmed to −20°C over 12 h, 4°C over 4 h, and room temperature over 4 h. After rinsing several times in acetone, the samples were removed from the sample holders and infiltrated in Spurr's resin in acetone using a 1:3, 1:1, and 3:1 (resin:acetone) infiltration series with incubations of 4 h in each solution. Samples were transferred twice to pure resin for 24 h, cast into 1-mL plastic capsules, and incubated at 60°C for 16 h.

Grid Preparation for Electron Microscopy

Nickel grids (200 mesh; Electron Microscopy Sciences) were washed in acetone for 5 min, ethanol for 5 min, and allowed to dry. A 0.2% (v/v) Formvar solution was prepared in dichloroethane and filtered. A glass slide was dipped into fresh Formvar solution, allowed to dry for 2 min at room temperature, and immersed in distilled water to allow the Formvar film to float to the surface. Cleaned grids were carefully placed onto the Formvar film, and the coated grids were collected with a strip of Parafilm and allowed to dry at room temperature.

Thin Sectioning for Electron Microscopy

Specimen blocks were trimmed to 1 mm^2 and sectioned to a thickness of 70 to 120 nm according to silver-gold refraction using 6.35-mm glass knives, cut at a 45° angle, on an Ultracut E ultramicrotome (Reichert-Jung, Vienna). Section compression was reduced using chloroform fumes.

Immunogold Labeling

Grids were blocked in 20 mM Tris-HCl, pH 7.5, 150 mM NaCl (TBS) containing 2% (w/v) BSA for 1 h, incubated with the primary antibody in a humid chamber for 2 h, and rinsed three times for 15 min each in TBS containing 2% (w/v) BSA and twice for 10 min each in TBS. Grids were

incubated for 1 h with 10 nm colloidal gold, goat anti-mouse IgG (Jackson Immunochemicals, West Grove, PA), and rinsed three times for 10 min each in TBS and twice for 10 min each in water. Grids were dried on filter paper before staining.

Grid Staining and Viewing

Cells fixed in osmium tetroxide and potassium permanganate were stained in 2% (w/v) uranyl acetate, 1% (w/v) lead citrate for 10 min in each solution. Immunogold-labeled grids were stained in a 4:1 2% (w/v) uranyl acetate:2% (w/v) potassium permanganate solution for 5 min. Grids were viewed at 75 kV using a Hitachi 7000X transmission electron microscope (Tokyo).

Fluorescence Microscopy and Imaging

Fluorescent tissues were viewed using a Leica DM RXA2 microscope (Leica Microsystems, Wetzlar, Germany) and images acquired with a Retiga EX digital camera (Qimaging, Burnaby, Canada). Deconvolution was performed using Open Lab version 2.09 (Improvision, Coventry, UK).

Sequence data from this article have been deposited with the EMBL/GenBank data libraries under accession numbers AF191772 (CYP80B1), AF025430 (BBE), and AF108432 (COR).

LITERATURE CITED

Achnine L, Blancaflor EB, Rasmussen S, Dixon RA (2004) Colocalization of L-phenylalanine ammonia-lyase and cinnamate 4-hydroxylase for metabolic channeling in phenylpropanoid biosynthesis. Plant Cell 16: 3098–3109

Allen RS, Millgate AG, Chitty JA, Thisleton J, Miller JAC, Fist AJ, Gerlach WL, Larkin PJ (2004) RNAi-mediated replacement of morphine with the non-narcotic alkaloid reticuline in opium poppy. Nat Biotechnol 22: 1559–1566

Amann M, Wanner G, Zenk MH (1986) Intracellular compartmentation of two enzymes of berberine biosynthesis in plant cell cultures. Planta 167: 310–320

Bauer W, Zenk MH (1989) Formation of both methylenedioxy groups in the alkaloid (S)-stylopine is catalyzed by cytochrome P-450 enzymes. Tetrahedron Lett 30: 5257–5260

Bauer W, Zenk MH (1991) Two methylenedioxy bridge forming cytochrome P-450 dependent enzymes are involved in (S)-stylopine biosynthesis. Phytochemistry 30: 2953–2962

Bird DA, Facchini PJ (2001) Berberine bridge enzyme, a key branch-point enzyme in benzylisoquinoline alkaloid biosynthesis, contains a vacuolar sorting determinant. Planta 213: 888–897

Bird DA, Franceschi VR, Facchini PJ (2003) A tale of three cell types: alkaloid biosynthesis is localized to sieve elements in opium poppy. Plant Cell 15: 2626–2635

Bock A, Wanner G, Zenk MH (2002) Immunocytological localization of two enzymes involved in berberine biosynthesis. Planta 216: 57–63

Bradford MM (1976) A rapid and sensitive method for the quantitation of microgram quantities of protein utilizing the principle of protein-dye binding. Anal Biochem 72: 248–254

Burbulis IE, Winkel-Shirley B (1999) Interactions among enzymes of the Arabidopsis flavonoid biosynthetic pathway. Proc Natl Acad Sci USA 96: 12929–12934

Campos F, Perez-Castineira JR, Villalba JM, Culianez-Marcia FA, Sanchez F, Serrano R (1996) Localization of plasma membrane H$^+$-ATPase in nodules of Phaseolus vulgaris L. Plant Mol Biol 32: 1043–1053

Cline SD, Coscia CJ (1989) Ultrastructural changes associated with the accumulation and secretion of sanguinarine in Papaver bracteatum suspension cultures treated with fungal elicitor. Planta 178: 303–314

Deliu C, Craciun C, Craciun V, Tamas M (1994) Ultrastructural and biochemical study of Berberis parvifolia root meristem and cell cultures. Plant Sci 96: 143–150

De Luca V, Cutler AJ (1987) Subcellular localization of enzymes involved in indole alkaloid biosynthesis in Catharanthus roseus. Plant Physiol 85: 1099–1102

Eilert U, Constabel F (1985) Ultrastructure of Papaver somniferum cultured in vitro and treated with fungal homogenate eliciting alkaloid production. Protoplasma 128: 38–42

Eilert U, Kurz WGW, Constabel F (1985) Stimulation of sanguinarine accumulation in Papaver somniferum cell cultures by fungal elicitors. J Plant Physiol 119: 65–76

Eilert U, Kurz WGW, Constabel F (1987) Ultrastructure of Catharanthus roseus cells cultured in vitro and exposed to conditions for alkaloid accumulation. Protoplasma 140: 157–163

Eilert U, Wolters B, Constabel F (1986) Ultrastructure of acridone alkaloid idioblasts in roots and cell cultures of Ruta graveolens. Can J Bot 64: 1089–1096

Facchini PJ (2001) Alkaloid biosynthesis in plants: biochemistry, cell biology, molecular regulation, and metabolic engineering applications. Annu Rev Plant Physiol Plant Mol Biol 52: 29–66

Facchini PJ, Johnson AG, Poupart J, De Luca V (1996a) Uncoupled defense gene expression and antimicrobial alkaloid accumulation in elicited opium poppy cell cultures. Plant Physiol 111: 687–697

Facchini PJ, Park SU (2003) Developmental and inducible accumulation of gene transcripts involved in alkaloid biosynthesis in opium poppy. Phytochemistry 64: 177–186

Facchini PJ, Penzes C, Johnson AG, Bull D (1996b) Molecular characterization of berberine bridge enzyme genes from opium poppy. Plant Physiol 112: 1669–1677

Froehlich JE, Itoh A, Howe GA (2001) Tomato allene oxide synthase and fatty acid hydroperoxide lyase, two cytochrome P450s involved in oxylipin metabolism, are targeted to different membranes of chloroplast envelope. Plant Physiol 125: 306–317

Galneder E, Rueffer M, Wanner G, Tabata M, Zenk MH (1988) Alternative final steps in berberine biosynthesis in Coptis japonica cell cultures. Plant Cell Rep 7: 1–4

Gerardy R, Zenk MH (1993a) Purification and characterization of salutaridine:NADPH 7-oxidoreductase from Papaver somniferum. Phytochemistry 34: 125–132

Gerardy R, Zenk MH (1993b) Formation of salutaridine from (R)-reticuline by a membrane-bound cytochrome P-450 enzyme from Papaver somniferum. Phytochemistry 32: 79–86

Giddings TH (2003) Freeze-substitution protocols for improved visualization of membranes in high-pressure frozen samples. J Microsc 212: 53–61

He XZ, Dixon RA (2000) Genetic manipulation of isoflavone 7-O-methyltransferase enhances biosynthesis of 4′-O-methylated isoflavonoid phytoalexins and disease resistance in alfalfa. Plant Cell 12: 1689–1702

Huang F-C, Kutchan TM (2000) Distribution of morphinan and benzo[c]phenanthridine alkaloid gene transcript accumulation in Papaver somniferum. Phytochemistry 53: 555–564

Jiang LW, Rogers JC (1998) Integral membrane protein sorting to vacuoles in plant cells: evidence for two pathways. J Cell Biol 143: 1183–1199

Johnson TL, Olsen LJ (2001) Building new models for peroxisome biogenesis. Plant Physiol 127: 731–739

Kutchan TM, Rush M, Coscia CJ (1986) Subcellular localization of alkaloids and dopamine in different vacuolar compartments of Papaver bracteatum. Plant Physiol 81: 161–166

Lenz R, Zenk MH (1995a) Acetyl coenzyme A:salutaridinol-7-O-acetyltransferase from Papaver somniferum plant cell cultures. J Biol Chem 270: 31091–31096

Lenz R, Zenk MH (1995b) Purification and properties of codeinone reductase (NADPH) from Papaver somniferum cell cultures and differentiated plants. Eur J Biochem 233: 132–139

Li XX, Franceschi VR, Okita TW (1993) Segregation of storage protein messenger-RNAs on the rough endoplasmic-reticulum membranes of rice endosperm cells. Cell 72: 869–879

Liu F, Cui XQ, Horner HT, Weiner H, Schnable PS (2001) Mitochondrial aldehyde dehydrogenase activity is required for male fertility in maize. Plant Cell **13:** 1063–1078

Lord JM (1983) Endoplasmic reticulum and ribosomes. *In* JL Hall, AL Moore, eds, Isolation of Membranes and Organelles from Plant Cells. Academic, Toronto, pp 119–134

Marrs KA (1996) The functions and regulation of glutathione *S*-transferase in plants. Annu Rev Plant Physiol Plant Mol Biol **47:** 127–158

McKnight TD, Bergey DR, Burnett RJ, Nessler CL (1991) Expression of enzymatically active and correctly targeted strictosidine synthase in transgenic tobacco plants. Planta **185:** 148–152

Morimoto S, Suemori K, Moriwaki J, Taura F, Tanaka H, Aso M, Tanaka M, Suemune H, Shimorhigashi Y, Shoyama Y (2001) Morphine in the opium poppy and its possible physiological function—biochemical characterization of the morphine metabolite, bismorphine. J Biol Chem **276:** 38179–38184

Mullen RT, Flynn CR, Trelease RN (2001) How are peroxisomes formed? The role of the endoplasmic reticulum and peroxins. Trends Plant Sci **6:** 256–261

Nakai K, Horton P (1999) PSORT: a program for detecting sorting signals in proteins and predicting their subcellular localization. Trends Biochem Sci **24:** 34–35

Nessler CL, Mahlberg PG (1977) Ontogeny and cytochemistry of alkaloidal vesicles in laticifers of *Papaver somniferum* L. (Papaveraceae). Am J Bot **64:** 541–551

Neve EPA, Ingelman-Sundberg M (2001) Identification and characterization of a mitochondrial targeting signal in rat cytochrome P450 2E1 (CYP2E1). J Biol Chem **276:** 11317–11322

Nielsen H, Engelbrecht J, Soren B, von Heijne G (1997) Identification of prokaryotic and eukaryotic signal peptides and prediction of their cleavage sites. Protein Eng **10:** 1–6

Ogishima T, Okada YOT, Omura T (1985) Import and processing of the precursor of cytochrome P-450 (SCC) by bovine adrenal cortex mitochondria. J Biochem (Tokyo) **98:** 781–791

Pan Z, Durst F, Werck-Reichhart D, Gardner HW, Camara B, Cornish K, Backhaus RA (1995) The major protein of guayule rubber particles is a cytochrome P450. Characterization based on cDNA cloning and spectroscopic analysis of the solubilized enzyme and its reaction products. J Biol Chem **270:** 8487–8494

Panicot M, Minguet EG, Ferrando A, Alcazar R, Blazquez A, Carbonell J, Altabella T, Koncz C, Tiburcio AF (2002) A polyamine metabolon involving aminopropyl transferase complexes in Arabidopsis. Plant Cell **14:** 2539–2551

Pauli HH, Kutchan TM (1998) Molecular cloning and functional heterologous expression of two alleles encoding (*S*)-*N*-methylcoclaurine 3′-hydroxylase (CYP80B1), a new methyl jasmonate-inducible cyto-

chrome P-450-dependent mono-oxygenase of benzylisoquinoline alkaloid biosynthesis. Plant J **13:** 793–801

Quitadamo IJ, Kostman TA, Schelling ME, Franceschi VR (2000) Magnetic bead purification as a rapid and efficient method for enhanced antibody specificity for plant sample immunoblotting and immunolocalization. Plant Sci **153:** 7–14

Rueffer M, Zenk MH (1987) Enzymatic formation of protopines by a microsomal cytochrome P-450 system of *Corydalis vaginans.* Tetrahedron Lett **28:** 5307–5310

Sakaguchi M, Mihara K, Sato R (1987) A short amino-terminal segment of microsomal cytochrome P-450 functions both as an insertion signal and as a stop-transfer sequence. EMBO J **6:** 2425–2431

Samanani N, Liscombe DK, Facchini PJ (2004) Molecular cloning and characterization of norcoclaurine synthase, an enzyme catalyzing the first committed step in benzylisoquinoline alkaloid biosynthesis. Plant J **40:** 302–313

Schmeller T, Latz-Brüning B, Wink M (1997) Biochemical activities of berberine, palmatine and sanguinarine mediating chemical defence against microorganisms and herbivores. Phytochemistry **44:** 257–266

Stevens LH, Blom TJM, Verpoorte R (1993) Subcellular localization of tryptophan decarboxylase, strictosidine synthase and strictosidine glucosidase in suspension-cultured cells of *Catharanthus roseus* and *Tabernaemontana divaricata.* Plant Cell Rep **12:** 573–576

St-Pierre B, De Luca V (1995) A cytochrome P-450 monooxygenase catalyzes the first step in the conversion of tabersonine to vindoline in *Catharanthus roseus.* Plant Physiol **109:** 131–139

Suzuki H, Koike Y, Murakoshi I, Saito K (1996) Subcellular localization of acyltransferases for quinolizidine alkaloid biosynthesis in *Lupinus.* Phytochemistry **42:** 1557–1562

Tanahashi T, Zenk MH (1990) Elicitor induction and characterization of microsomal protopine-6-hydroxylase, the central enzyme in benzophenanthridine alkaloid biosynthesis. Phytochemistry **29:** 1113–1122

Unterlinner B, Lenz R, Kutchan TM (1999) Molecular cloning and functional expression of codeinone reductase: the penultimate enzyme in morphine biosynthesis in the opium poppy *Papaver somniferum.* Plant J **18:** 465–475

Widholm JM (1972) The use of fluorescein diacetate and phenosafranine for determining viability of cultured plant cells. Stain Technol **47:** 189–194

Wink M, Hartmann T (1982) Localization of the enzymes of quinolizidine alkaloid biosynthesis in leaf chloroplasts of *Lupinus polyphyllus.* Plant Physiol **70:** 74–77

Yamamoto H, Nakagawa K, Fukui H, Tabata M (1986) Cytological changes associated with alkaloid production in cultured cells of *Coptis japonica* and *Thalictrum minus.* Plant Cell Rep **5:** 65–68